



HAL
open science

Do transparent exopolymeric particles (TEP) affect the toxicity of nanoplastics on *Chaetoceros neogracile*?

Carmen González-Fernández, Jordan Toullec, Christophe Lambert, Nelly Le Goïc, Marta Seoane, Brivaëla Moriceau, Arnaud Huvet, Mathieu Berchel, Dorothée Vincent, Lucie Courcot, et al.

► To cite this version:

Carmen González-Fernández, Jordan Toullec, Christophe Lambert, Nelly Le Goïc, Marta Seoane, et al.. Do transparent exopolymeric particles (TEP) affect the toxicity of nanoplastics on *Chaetoceros neogracile*?. *Environmental Pollution*, 2019, 250, pp.873-882. 10.1016/j.envpol.2019.04.093. hal-02130232

HAL Id: hal-02130232

<https://hal.science/hal-02130232>

Submitted on 15 Jun 2020

HAL is a multi-disciplinary open access archive for the deposit and dissemination of scientific research documents, whether they are published or not. The documents may come from teaching and research institutions in France or abroad, or from public or private research centers.

L'archive ouverte pluridisciplinaire **HAL**, est destinée au dépôt et à la diffusion de documents scientifiques de niveau recherche, publiés ou non, émanant des établissements d'enseignement et de recherche français ou étrangers, des laboratoires publics ou privés.

Do transparent exopolymeric particles (TEP) affect the toxicity of nanoplastics on *Chaetoceros neogracile*?

González-Fernández Carmen⁵, Toullec Jordan¹, Lambert Christophe⁵, Le Goïc Nelly⁵, Seoane Marta, Moriceau Brivaela⁵, Huvet Arnaud², Berchel Mathieu³, Vincent Dorothée⁴, Courcot Lucie⁴, Soudant Philippe⁵, Paul-Pont Ika^{5,*}

¹ Laboratoire des Sciences de L'Environnement Marin (LEMAR), UMR 6539 CNRS/UBO/IRD/IFREMER, Institut Universitaire Européen de La Mer (IUEM), Rue Dumont D'Urville, 29280, Plouzané, France

² Ifremer, Laboratoire des Sciences de L'Environnement Marin (LEMAR), CS 10070, 29280, Plouzané, France

³ CEMCA, UMR CNRS 6521, IBSAM, UFR Sciences, Université de Bretagne Occidentale, 6 Avenue Victor Le Gorgeu, 29238, Brest, France

⁴ Univ. Littoral Côte D'Opale, Univ. Lille, CNRS, UMR 8187, LOG, Laboratoire D'Océanologie et de Géosciences, 32 Avenue Foch, F-62930, Wimereux, France

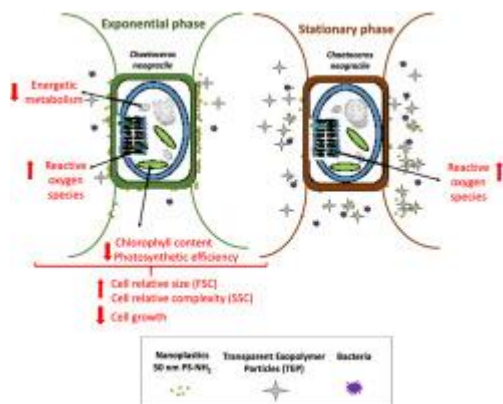
⁵ CNRS

* Corresponding author : Paul-Pont Ika, email address : ika.paulpont@univ-brest.fr

Abstract :

The potential presence of nanoplastics (NP) in aquatic environments represents a growing concern regarding their possible effects on aquatic organisms. The objective of this study was to assess the impact of polystyrene (PS) amino-modified particles (50 nm PSNH₂) on the cellular and metabolic responses of the diatom *Chaetoceros neogracile* cultures at two essential phases of the growth cycle, i.e. exponential (division) and stationary (storage) phases. Both cultures were exposed for 4 days to low (0.05 µg mL⁻¹) and high (5 µg mL⁻¹) concentrations of PS-NH₂. Exposure to NP impaired more drastically the major cellular and physiological parameters during exponential phase than during the stationary phase. Only an increase in ROS production was observed at both culture phases following NP exposures. In exponential phase cultures, large decreases in chlorophyll content, esterase activity, cellular growth and photosynthetic efficiency were recorded upon NP exposure, which could have consequences on the diatoms life cycle and higher food-web levels. The observed differential responses to NP exposure according to culture phase could reflect i) the higher concentration of Transparent Exopolymer Particles (TEP) at stationary phase leading to NP aggregation and thus, probably minimizing NP effects, and/or ii) the fact that dividing cells during exponential phase may be intrinsically more sensitive to stress. This work evidenced the importance of algae physiological state for assessing the NP impacts with interactions between NP and TEP being one key factor affecting the fate of NP in algal media and their impact to algal cells.

Graphical abstract



Highlights

► Interaction of NP and diatoms was studied at exponential and stationary phases. ► Transparent Exopolymer Particles (TEP) alter NP fate by aggregating NP. ► NP impairs major physiological traits of diatoms at exponential phase. ► Whatever the aggregation state, NP promotes oxidative stress at both growth phases.

Keywords : nanoplastics, diatoms, physiology, transparent exopolymer particles

46 **1. Introduction:**

47 Marine plastic pollution is a major environmental concern. Plastics have an increasing
48 global production (>320 million tons of plastics; Plastic Europe 2017) and a part of this
49 production ends up as waste in the Oceans. Small plastic particles (diameter < 5mm)
50 called microplastics (MP) have been found in waters and sediments around the world,
51 reaching concentrations of 8.5 mg L⁻¹ and 33.0 mg kg⁻¹ respectively (MP sizes ranging
52 between 1 and 275µm) in the most polluted areas (Bergmann et al., 2017; Dubaish and
53 Liebezeit., 2013). However, as a result of the technical limitation for their identification,
54 little attention has been paid to small microparticles, and notably the nanoplastics
55 fraction (GESAMP, 2016). Nanoplastics (NP) were considered as plastic particles that
56 are <100 nm in the definition of engineered nanomaterials (Mattsson et al., 2015;
57 GESAMP, 2016). Primary NP are produced for a wide range of applications such as
58 biosensors (Velev and Kaler, 1999), photonics (Rogach et al., 2000), nanocomposites
59 (Merinska and Dujkova, 2012) and drug delivery tools and cosmetics (Hernandez et al.,
60 2017) as well as pharmaceutical products (FAO, 2017) while secondary NP may
61 originate as demonstrated experimentally from mechanical fragmentation (Lambert and
62 Wagner, 2016), photo-degradation (Gigault et al., 2016) or biodegradation (Dawson et
63 al., 2018) of larger items. NP have been estimated as one of the largest share of
64 nanomaterials on the market (Fabra et al., 2013) and their first report in the aquatic
65 environment was argued in the North Atlantic Gyre (Ter Halle et al., 2017).

66 Amongst phytoplankton, diatoms represent one of the most abundant group, recognized
67 to be responsible for around 40% of global primary productivity in the oceans (Malviya
68 et al., 2016) and influencing the global carbon cycle (Field et al., 1998). The interaction
69 between MP and marine diatom aggregates has already been shown experimentally
70 (Long et al., 2015; 2017) modifying both algae and MP settlement rates in the water
71 column. Due to their intrinsic characteristics, nanomaterials, and more often NP, may
72 have higher impact than their micro-scale counterparts (Mao et al., 2018).
73 Phytoplankton cell walls constitute the first barrier for uptake encountered by any
74 substances including nanoparticles (Khowala et al., 2008). Nanoplastics can attach to
75 the cell surfaces as suggested for the green microalgae *Dunaliella tertiolecta* (Bergami
76 et al., 2017; Nolte et al., 2017) while crossing the cell wall will depend on the size:
77 nanoplastics with larger size than cell wall pore (> 20 nm for diatoms) will not easily
78 cross cell wall (Navarro et al., 2008).

79 In recent years, the impact of NP on freshwater algae physiology (e.g. photosynthesis)
80 has raised controversial results. On the one hand, studies revealed a decrease in algal
81 photosynthesis upon polystyrene nano-beads exposure (Bergami et al., 2017;
82 Bhattacharya et al., 2010; Mao et al., 2018). On the other hand, other studies reported
83 decreased algal growth with no impact on algal photosynthetic rate (Sjollema et al.,
84 2016; Yokota et al., 2017). Due to technical limitation for its characterization, the
85 assessment of NP behavior in natural environments is still a challenge. Nevertheless,
86 interactions of NP amongst themselves and with other macromolecules such as
87 polysaccharide, organic matter, proteins between others, have been already evidenced
88 under laboratory conditions (Canesi et al., 2017; Galloway et al., 2017) and it is directly
89 related to their toxicity for organisms (reviewed in Paul-Pont et al., 2018). Diatoms (and
90 bacteria) are well known for excreting large quantities of Exopolymeric Substances
91 (EPS) during their growth. One type of EPS called Transparent Exopolymer Particles
92 (TEP) has received increasing attention because of their high stickiness (Passow, 2002).
93 Thus, TEP may interact with NP in natural environments. In fact, differential production
94 of carbohydrates by micro-algae was already observed (Lagarde et al., 2016) depending
95 on the chemical composition of the MP to which they were exposed. Hence, higher
96 carbohydrate production was related to high density polyethylene compared to
97 polypropylene. In addition, TEP is not species-specific (Allard and Tazi, 1993) and
98 rather depends on the age of the strain and/or external conditions such as the presence of
99 bacteria (Corzo et al., 2000). In this context, we hypothesized that physiological state of
100 microalgae may play a role in NP fate and toxicity depending on TEP concentration in
101 the culture media and their interactions with NP.

102 In this work, we studied the effects of NP (50 nm) exposure on the cellular and
103 metabolic responses of the diatom *Chaetoceros neogracile* during exponential and
104 stationary culture phases via a single experimental design. This has never been assessed
105 before and is of major importance to advance knowledge in the impacts of plastic debris
106 in marine ecosystems. Two concentrations of NP were used: a high concentration ($5 \mu\text{g}$
107 mL^{-1}) established to compare results with other laboratory ecotoxicological studies (e.g.
108 Bergami et al., 2017; Nolte et al., 2017) and a 100 times lower concentration ($0.05 \mu\text{g}$
109 mL^{-1}) to get closer to suspected concentrations in highly contaminated environment
110 (Huvet et al., 2016; Lenz et al., 2016). Taking into account the relevance of the
111 surrounding media on NP fate and their potential toxicity (Canesi et al., 2017; Galloway

112 et al., 2017), TEP concentration in the culture media was quantified and NP aggregation
113 in algae' media was characterized.

114 **2. Material and methods**

115 2.1. Batch culture setups

116 Batch cultures of non-motile diatom *Chaetoceros neogracile* (width: 4 μ m, length: 7 μ m;
117 strain CCAP 1010-3) were done in 500 mL flasks containing 400 mL of sterilized
118 filtered (0.2 μ m) seawater (FSW) including 1 mL L⁻¹ of silica and Conway's medium
119 (Walne, 1966) in a 24 h light cycle with a constant intensity of 100 μ moles photons m⁻²
120 s⁻¹ at adjusted room temperature of 20°C. Flasks were kept in constant aeration and CO₂
121 was supplied to keep the pH between 7.5-7.9. Two sets of cultures were prepared at 7
122 days interval in order to expose simultaneously *C. neogracile* in exponential phase (3
123 days old) and in stationary phase (10 days old) to NP. The growth phases were validated
124 previously thanks to a calculation of a growth curve under same conditions of the
125 experiment (data not shown).

126 2.2. Nanoplastics characterization

127 Fluorescent-blue 50 nm polystyrene amino (PS-NH₂) nanoparticles were purchased
128 from Sigma-Aldrich (Saint Louis, USA) with an Excitation/Emission: 358 nm/410 nm.
129 Physico-chemical characteristics of NP were confirmed in ultrapure water. Size (Z-
130 average), charge and aggregation state (polydispersity index, PdI) of NP were
131 determined by Dynamic Light Scattering (DLS) using a nano-Zetasizer (Malvern
132 instruments, United Kingdom). Measurements were performed in triplicates, each
133 containing 13 runs for the Z-average and 40 runs for Z-potential. In addition, NP shape
134 was also characterized in ultrapure water by transmission electronic microscopy
135 (JeolJEM 100 CX II). In brief, nanoplastics were diluted in ultrapure water (100 μ g mL⁻¹)
136 and placed on copper grid (400 nm mesh) with a carbon-coated Formvar film
137 (Polysciences) and marked with 2% (wt/vol) uranyl acetate to be measured.

138 DLS analyses of NP were also performed in FSW and algae' spent media of both
139 cultures (exponential and stationary cultures). Algae' spent media were obtained after
140 centrifugation of an algal culture (stationary or exponential) at 550 g for 5 min and
141 supernatant was collected. Data were analyzed using Zetasizer Nano Series software,
142 version 6.20. Results are presented as mean (n=3) \pm standard deviations.

143 2.3. Exposure

144 To keep cells in the same culture exposure conditions (i.e. in exponential and stationary
145 growths), concentrations of both batch cultures were adjusted at 4×10^5 cells mL⁻¹ by
146 centrifugation (550 g for 5 minutes, final volume 300 mL) and resuspended in their
147 respective media (exponential or nutrient replete vs. stationary media or nutrient
148 limited). This was performed to obtain the same cell/NP ratio without having to dilute
149 algae culture with FSW which could have introduced a bias (dilution of nutrients,
150 exudates, etc.).

151 For each culture phase (stationary and exponential), three experimental treatments were
152 designed: control (no addition of NP), low NP concentration (0.05 µg mL⁻¹) and high
153 NP concentration (5 µg mL⁻¹). All treatments (control, low and high) were performed in
154 triplicates for each culture phase (exponential and stationary). *Chaetoceros neogracile*
155 cultures were sampled after 4, 24, 48, 72 and 96 h exposure to perform the following
156 analyses.

157 2.4. Analyses

158 2.4.1. Scanning electron microscope visualization of NP–diatoms interactions

159 For scanning electron microscopy (SEM) observations, only cultures in exponential
160 phase, which were significantly affected by NP, were analyzed. After 72 h exposure,
161 one mL sample of each replicate from control and high NP treatments was fixed in
162 pseudo-lugol (2% final) according to Verity et al. (2007) protocol, which had proved to
163 be a good fixative for diatoms' cells and store at 4°C until analysis. In parallel,
164 additional tests were performed to compare the quality of SEM analyses between fresh
165 and pseudo-lugol fixed samples as we had no clue on the potential effect of pseudo-
166 lugol on the physical interaction between NP and diatom cells.

167 Nevertheless, gradual or direct dehydration with ethanol from Lugol's solution caused
168 gross shrinkage (Bistricki and Munawar, 1978). Thus, both, fresh and pseudo-lugol
169 fixed samples were fixed and post-fixed, respectively, in 0.1 M sodium cacodylate
170 buffer (1.75% w/v of NaCl, pH 7.2) for 10 min at 4 °C before being filtered through
171 polycarbonate filters with a 2 µm pore size. Later, filters were rinsed with a solution of
172 sodium cacodylate 0.1 M (2% w/v of NaCl) in ultrapure water. Samples were then
173 dehydrated by successive immersions in alcoholic hexamethyldisilazan (HMDS) (v:v):

174 absolute ethanol–HMDS (3:1), absolute ethanol–HMDS (1:1), absolute ethanol–HMDS
175 (1:3), and pure HMDS. Finally, samples were coated with gold palladium before being
176 observed by SEM (Hitachi S-3200N).

177 2.4.2. Algae descriptive and physiological parameters and bacteria concentration

178 Flow cytometric analyses were performed in triplicates in each experimental treatment
179 and algal stage using an EasyCyte Plus cytometer (Guava Technologies, Millipore,
180 Billerica, MA), equipped with a 488-nm argon laser and three fluorescence detectors:
181 green (GRN 525/30 nm), yellow (YLW 583/26 nm), and red (RED 680/30 nm).
182 Parameters measured by flow cytometry (cell number and descriptive parameters,
183 microalgal chlorophyll a content, esterase activity, intracellular Reactive Oxygen
184 Species (ROS) production and Bacteria concentration) were measured on separated
185 aliquots according to the following protocols:

186 ***Cell number and descriptive parameters.*** Cells were detected on the flow-cytometer by
187 their optical characteristics obtained at small angle (Forward scatter, FSC) and large
188 angle (Side Scatter, SSC). The flow-cytometer is equipped with an absolute counting
189 system (peristaltic pump, flow rate) allowing calculation of the algae' concentration,
190 expressed in cell mL⁻¹.

191 ***Microalgal chlorophyll a content*** was estimated using chlorophyll autofluorescence
192 from the selected microalgal population (RED detector of the flow-cytometer, 680/30
193 nm; Long et al. 2017). Data was expressed as the mean of red fluorescence per cell in
194 arbitrary units (A.U.).

195 ***Esterase activity*** which is considered as a proxy of primary metabolism (Garvey et al.,
196 2007) was measured using the fluorescein diacetate staining (FDA; Invitrogen # F1303;
197 final concentration 6 µM) incubating samples for 10 min at 18 °C in the dark. FDA is a
198 nonpolar compound that can permeate into the cells. Once inside the cells, FDA is
199 cleaved by esterases into acetate and fluorescein molecules (fluorescent green) which
200 are retained within the cells. Intracellular fluorescence increases with both metabolic
201 activity and time. Esterase activity was estimated by measuring the level of green
202 fluorescence (GRN detector of the flow-cytometer) and expressed as mean of
203 fluorescence per cell in arbitrary units (A.U.). Esterase activity was measured at all time

204 for the stationary phase culture and after 4, 24, 48, 96 h for the exponential phase
205 culture.

206 **Intracellular Reactive Oxygen Species (ROS) production** was measured using 2,7-
207 dichlorofluorescein diacetate (DCFH-DA; Sigma-Aldrich, D6883; final concentration
208 10 μM) after 50 min of incubation at 18 °C in the dark (Long et al. 2017). DCFH is
209 hydrolyzed (esterase) intracellularly to form DCF which produces green fluorescent
210 upon oxidation with ROS. The green fluorescence measured (GRN detector of the flow-
211 cytometer) is quantitatively related to the intracellular ROS production and is expressed
212 as the mean of green fluorescence per cell in arbitrary units (A.U.).

213 **Bacteria concentration** (adapted from Marie et al., 1997) was measured in each culture
214 flask (n=3 for each treatment) in both exponential and stationary cultures, at the
215 beginning and the end of the experiment, by fixing 500 μL of algae culture with
216 formaldehyde (0.35% final) for 10 minutes at room temperature in the dark before
217 freezing the samples (-20 °C) until analysis. Samples were 1/10 diluted in filtered sterile
218 seawater and incubated for 10 min in the dark after addition of 5 μL of SYBR® Green I
219 commercial solution (Molecular Probes, #S7563) diluted at 1/100 in Milli-Q water.
220 SYBR® Green I was used to detect bacteria as it stains DNA which fluorescence green
221 and was detected by FL1 detector. Results are given as concentration of bacteria in cells
222 per mL. Additionally, bacteria load (bacteria by cell) was also calculated dividing
223 bacteria concentration by cell concentration.

224 **Photosynthetic efficiency (F_v / F_m)** which is a proxy of PSII photochemical efficiency,
225 was measured by pulse amplitude modulation (PAM) fluorometry with a handled
226 AquaPen-C AP-C 100 (Photon Systems Instruments, Drassov, Czech Republic)
227 equipped with a blue light (455 nm). For each sampling time, 3 mL sample of each
228 culture were dark-adapted for 30 minutes before measurement of fluorescence variables
229 (F_0 , F_m , F_v). F_0 is the initial fluorescence intensity, F_m the maximal intensity under
230 saturating light conditions, and $F_v = F_m - F_0$ (Strasser et al., 2000).

231 **Transparent Exopolymer Particles (TEP) concentration** was measured following the
232 method developed by Passow and Alldredge (1995). Three to five replicates were
233 sampled from each culture before the exposure. Later, samples were prepared for
234 exposure as described in section 2.3. At the end of the experiment (96 h exposure), a
235 concentration of 1×10^4 cells mL^{-1} of each culture flask were filtered onto 0.4 μm

236 polycarbonate filters under low vacuum pressure and stained with 0.5 mL Alcian blue
237 solution (0.02 % in aqueous solution, 0.06 % acetic acid, pH 2.5, filtered at 0.2 μm
238 before use). Polycarbonate filters were then soaked for 2 h in 6 mL of 80 % H_2SO_4
239 solution under agitation. The absorption of the obtained solution was measured at 787
240 nm in a 1 cm cuvette and was converted in gram of Gum Xanthan equivalent per liter
241 (g Xeq L^{-1}) using a Gum Xanthan calibration curve fitting our working Alcian blue
242 solution.

243 2.5. Statistical analyses

244 Statistical analysis was performed using STATGRAPHICS centurion XV.II (Statpoint
245 Technologies, Inc. Warrenton, Virginia, USA). Differences were considered significant
246 at $p < 0.05$. Normality and homogeneity of variances of the data distribution were tested
247 by standardized skewness and standardized kurtosis and Levene's test, respectively.
248 One-way-ANOVA analysis was performed to establish significant differences between
249 treatments at each time. A Tukey's post hoc test was used to test differences among the
250 different exposure treatments. Arcsine or log transformation was performed when
251 necessary to meet the normality and homoscedasticity criteria. Non-parametric analysis
252 (Kruskal-Wallis test) was also performed when the variables did not meet the
253 requirements of a parametric ANOVA.

254 3. Results

255 3.1. Nanoplastics behavior and fate in culture media

256 DLS analysis confirmed the expected size of NP in ultrapure water, with a Z-average of
257 53.5 ± 0.2 nm (Figure 1A). Nanoparticle geometric diameter was also confirmed in
258 ultrapure water using transmission electron microscopy (Fig. 1E). In FSW, size of NP
259 was similar (55.1 ± 0.5 nm; Fig. 1B). Aggregation was negligible as suggested by a
260 $\text{PdI} < 0.2$ for both ultrapure and FSW conditions.

261 Results of NP size and aggregation state monitored in the filtered spent media of algae
262 cultures revealed a moderate aggregation, showing a size of 70.5 ± 2.2 nm ($\text{PdI} = 0.3 \pm$
263 0.0) and 162.4 ± 3.3 nm ($\text{PdI} = 0.6 \pm 0.0$) at exponential and stationary phases,
264 respectively (Fig. 1C and 1D).

265 Regarding the charge, NP resuspended in ultrapure water had a strong positive charge
266 45.4 ± 0.2 mV but was reduced to 14.3 ± 3.5 mV when resuspended in FSW. Similarly
267 to FSW, NP resuspended in both exponential and stationary spent media had a positive
268 charge reduced down to 11.0 ± 4.4 mV and 17.5 ± 4.3 mV, respectively.

269 3.2. Adhesion of nanoplastics to algae cells.

270 SEM observations were performed to visualise the diatom cells structure and assess
271 potential impacts of NP exposure on cell shape and integrity. Fresh cells of control
272 cultures of *Chaetoceros neogracile* in exponential phase presented intact silica frustule
273 and setae (Figure 2A; 2B). Sometimes, the setae were broken and situated close to the
274 cell as a consequence of the force exerted during filtration process (sampling
275 preparation; e.g. in Fig.2B). Control samples fixed in pseudo-Lugol evidenced more
276 deteriorated frustules compared to fresh samples (Supplementary Figure 1).

277 After exposure to nanoplastics, adsorption of nanoplastics onto algal' cell surface was
278 observed in both fresh (Fig. 2C and 2D) and pseudo-lugol' fixed (Supp. Fig 1) samples.
279 Pseudo-lugol fixed samples evidenced large amount of aggregated debris in cells
280 exposed to NP (Supp. Fig 1), but not in controls. However, this amount of debris was
281 not observed in any of the fresh samples regardless of the experimental condition
282 considered (including high NP concentration), suggesting that fixation promoted higher
283 debris aggregation when NP are present.

284 3.3. Phytoplankton responses to nanoplastics exposure

285 3.3.1. Cell growth

286 In control treatments (no addition of NP), culture growth was higher in exponential
287 phase in comparison with stationary phase, with final cellular concentrations being 2
288 and 19 times higher than at the beginning of the experiment in stationary and
289 exponential growth phases, respectively (Supplementary table 1).

290 Exposure to high NP concentration significantly reduced cell growth of culture in
291 exponential phase. Growth rate was reduced by 49, 57 and 62 % compared to controls
292 after 48, 72 and 96 h of exposure, respectively (Figure 3A; ANOVA; $p < 0.01$). No
293 significant effect on cell growth was observed at low NP concentration (Figure 3A).

294 The low growth of cultures in stationary phase was not affected by NP exposure
295 regardless of the NP concentration and exposure duration (Supp. Table 1).

296 3.3.2. Changes in cell's optical characteristics

297 Exposure of culture in exponential phase to high NP concentration resulted in up to 100
298 % increase of cells' optical characteristics at large angle (Side Scatter, SSC). After 4 h
299 exposure, SSC increased by 35% compared to controls. This increase was also observed
300 during the rest of the experiment (ANOVA; $p < 0.001$ all exposure durations; Fig. 3B).
301 Conversely, cell exposed to low NP concentration did not show any modification of
302 their SSC, although a significant 5 % increase of Forward Scatter (FSC) as compared to
303 controls was detected after 96 h exposure (ANOVA; $p < 0.01$; Fig. 3C).

304 3.3.3. Chlorophyll a content

305 In cultures in exponential phase, an 8 % decrease in chlorophyll a content compared to
306 controls was observed after 4 and 24 h exposure at both NP concentrations (ANOVA; p
307 < 0.05). For respectively low and high NP exposures, the reductions reached 9 and 24 %
308 after 48 h exposure, 6 and 33 % after 72 h exposure and 14 and 32 % after 96 h
309 exposure. For cultures in stationary phase, no significant effect of NP exposure was
310 observed on chlorophyll a content regardless of the NP concentrations and exposure
311 duration (Fig 3D; Supp. Table 2).

312 3.3.4. Photosynthetic efficiency

313 Photosynthetic efficiency of cells in exponential phase decreased after 4 h exposure
314 with a reduction of 2 and 3 % for low and high NP concentrations, respectively
315 (ANOVA; $p < 0.01$ both NP concentrations). After 48 h exposure, the photosynthetic
316 efficiency was reduced by 13% only at high NP concentration until the end of the
317 experiment (ANOVA; $p < 0.001$; Fig. 3E). In cultures in stationary phase, a significant
318 decrease in photosynthetic efficiency was observed at low NP concentration after 4 h
319 exposure (ANOVA; $p < 0.01$) being 6 % lower than control. No significant effect of NP
320 exposure was recorded on photosynthetic efficiency thereafter (Supp. Table 2).

321 3.3.5. Esterase activity

322 A significant decrease in esterase activity was observed in cultures in exponential phase
323 showing values of 8 % and 21 % reductions after 4 h (ANOVA; $p < 0.05$) for low and

324 high NP exposure, respectively. A reduction of this parameter was also observed after
325 24 h exposure (24 % and 52 % decrease at low and high NP concentration,
326 respectively), 48 h exposure (17 % and 69 % decrease at low and high NP
327 concentration, respectively), and 96 h exposure (19 % and 38 % decrease at low and
328 high NP concentration, respectively) (ANOVA; $p < 0.001$ all times; Fig 3F). No
329 significant effect of NP exposure on esterase activity of culture in stationary phase was
330 observed (Supp. Table 2).

331 3.3.6. Intracellular ROS production

332 Nanoplastics exposure triggered a significant increase in intracellular ROS production
333 of *C. neogracile* at both culture phases and both NP concentrations (Supp. Table 2).
334 Cultures at exponential phase exposed to high NP concentration showed an increase in
335 ROS production by 48% after 4 h exposure (ANOVA; $p < 0.05$) and reaching 22 %
336 after 48 and 72 h exposure (ANOVA; $p < 0.001$ both exposure times; Fig 3G).

337 Cultures in stationary phase evidenced an increase in ROS production at both NP
338 concentrations, around 12 % and 14 % at low and high NP concentrations, respectively,
339 compared to the control after 4 h, 48 h and 72 h of exposure (ANOVA; $p < 0.05$ all
340 exposure times).

341 3.3.7. Bacteria concentration in the cultures

342 At the beginning of the experiment the bacteria load was 14 times higher in cultures in
343 stationary phase (values bacteria cell⁻¹) than in exponential phase (values bacteria cell⁻¹)
344 (ANOVA; $p < 0.001$).

345 At the end of the experiment, bacteria concentration was still twice higher in culture in
346 stationary phase (ANOVA; $p < 0.01$) as compared to exponential ones. At this time, a
347 significant reduction of bacteria concentration by 30.5 % was observed at high NP
348 concentration in the culture in exponential phase (ANOVA; $p < 0.01$) compared to
349 control. However, when normalized by the diatom cell concentration in this culture,
350 bacteria load at high NP concentration (4 bacteria cell⁻¹) was two times higher than in
351 controls (ANOVA; $p < 0.01$) (Fig. 3H). Neither bacteria concentration nor bacteria-
352 diatom ratio in stationary cultures were significantly affected by NP exposures (Fig.
353 3H).

354 3.3.8. Concentration of Transparent Exopolymer Particles (TEP)

355 At the beginning of the experiment, TEP concentration was 5 times higher in *C.*
356 *neogracile* cultures in stationary phase than in cultures in exponential phase ($5.5 \times 10^4 \pm$
357 1.2×10^3 and $1.1 \times 10^4 \pm 1.3 \times 10^3$ $\mu\text{g Xeq L}^{-1}$ in stationary and exponential phases,
358 respectively) as presented in Figure 4A. When normalized by the diatom cell number
359 (Fig. 4B), TEP were 2 times more concentrated in *C. neogracile* cultures in exponential
360 phase than in stationary phase, (~ 6 μg and ~ 3 $\mu\text{g Xeq Cell}^{-1}$ in exponential and
361 stationary phases, respectively).

362 At the end of the experiment, TEP concentration in exponential phase exposed to high
363 NP concentration was 2.3 times reduced as compared to controls (1.5×10^4 and 3.5×10^4
364 $\mu\text{g Xeq L}^{-1}$ for high NP exposure and control conditions, respectively, Figure 4C).
365 However, when normalized by the diatom cell concentration, the same final TEP
366 concentration per cell was observed in exponential cultures for all treatments (control,
367 low NP, high NP: ~ 3 $\mu\text{g Xeq Cell}^{-1}$, Figure 4D). At this time for cultures in stationary
368 phase, no differences in TEP concentration between treatments were observed either in
369 $\mu\text{g Xeq L}^{-1}$ ($\sim 1.56 \times 10^4 \pm 3.1 \times 10^2$ $\mu\text{g Xeq L}^{-1}$) or normalized per diatom cell (~ 18 μg
370 Xeq Cell^{-1}) (Fig. 4C; 4D).

371

372 **4. Discussion:**

373 The main objective of this work was to identify the effect of small nanoplastics (50 nm)
374 on the cellular and metabolic responses of a diatom, *Chaetoceros neogracile*, at two
375 growth phases (exponential and stationary growth phases) via a single experimental
376 design. This experimental approach is innovative and has been never performed before.
377 Moreover, the present study include the measurement of bacteria and TEP
378 concentrations in algae media, as well as characterization of NP behavior in algal
379 cultures, thus providing useful information about the impact of NP on diatoms at
380 different growth phases.

381 **Transparent Exopolymer Particles (TEP) concentration influences NP fate**

382 According to recent findings, components present in water such as colloids and natural
383 organic matter, under a variety of physico-chemical conditions including pH and ionic
384 strength, affect significantly NP behavior, fate and toxicity (Manfra et al., 2017;

385 reviewed in Paul-Pont et al., 2018). Plastics has been proven to rapidly develop in its
386 hydrophobic surface diverse microbial community of heterotrophs, autotrophs,
387 predators, and symbionts not found in other substrates in the upper layer of oceans
388 (Datta et al., 2016). This specific plastic associated communities were termed the
389 “*plastisphere*” by Zettler et al. (2013) and evidenced the high adhesion capacity of
390 plastics in natural environments.

391 Diatoms are particularly well known for excreting significant quantities of
392 exopolysaccharides (EPS) that may rearrange to form larger particles, the TEP (Mari et
393 al., 2017). TEP are essentially constituted by polysaccharides highly surface-active,
394 enriched in deoxysugars and covalently bound sulfate (Mopper et al., 1995; Zhou et al.
395 1998), with a strong tendency to form metal ion bridges and hydrogen bonds (Passow
396 2002). These highly sticky particles trigger aggregation of various organic and mineral
397 solid particles from natural or anthropogenic origin (Mari et al. 2017; Long et al. 2015;
398 Passow and De La Rocha, 2006; Zhao et al. 2017). Despite TEP’ low density (lower
399 than sea-water) that sometimes lead to form ascending particles, TEP adhesion capacity
400 are so high that most aggregates formed in the natural environment contained a large
401 proportion of ballasted particles associated to strong sinking and export to deeper layer
402 (Azetsu-Scott and Passow, 2004; Mari et al. 2017; Long et al. 2015). This explained
403 why TEP can easily interact with NP, as it has been evidenced with MP (Long et al.
404 2017; Zhao et al. 2017). In our work, a moderate aggregation of NP was observed in
405 diatoms spent media, but neither in filtered seawater nor in ultrapure water. This may be
406 linked to the formation of an environmental coating, or ‘eco-corona’ around NP as
407 previously described (Canesi et al. 2017; Galloway et al., 2017). Although the nature of
408 the eco-corona was not investigated, the influence of TEP in the formation of moderate
409 aggregates is suggested here in accordance with previous findings (Long et al. 2015;
410 Lagarde et al. 2016). TEP appear to act as binding agent, holding plastic particles
411 together into agglomerates as it was previously reported for 50 nm polystyrene particles
412 in the presence of exopolymeric substances (EPS; Summers et al., 2018). In our work,
413 total TEP concentration at the beginning of the experiment at stationary phase was 5
414 times higher than in exponential phase. TEP concentration generally increase when
415 nutrient limit cell growth as also occurred in natural environment where TEP
416 accumulate in surface waters at the end of bloom (Passow 2000, 2002, Mari et al. 2017).
417 As EPS are also excreted by bacteria, the increase of TEP measured in our experiment
418 may also be due to the high bacteria load observed at stationary growth. This bacteria

419 load not only can participate in TEP production but also get involved in the
420 “*plastisphere*” of NP depending on plastic type and mostly on environmental conditions
421 (Summers et al., 2018).

422

423 Regardless of their origin, presence of TEP in the media promoted aggregation of NP.
424 The resulting increase in particle size may have affected their toxicity (Paul-Pont et al.,
425 2018). Indeed, previous studies reported that micro-scale ($>1\mu\text{m}$) particles had less
426 impact on microalgae than nano-scale plastics (Mao et al., 2018; Sjollemma et al., 2016).
427 In addition to the particle size, significant lower values of NP zeta potential were
428 observed in both FSW and algae media. Decrease in positive charges of NP in FSW has
429 been already reported (Bergami et al., 2016) due to interaction of the surface groups
430 with high number of ions (Cole and Galloway, 2015). However, the presence of TEP
431 did not appear to further alter the behavior and fate of NP as compared to FSW.

432 Altogether, NP aggregation and charge reduction could have minimized NP impacts as
433 observed in this study for cultures in stationary phase.

434 **NP affected the concentration of Transparent Exopolymer Particles (TEP)**

435 The presence of exopolymeric substances (EPS) produced by microalgae and bacteria is
436 associated to diatom cell stickiness and subsequent aggregation, which have an
437 important role in the redistribution and export of organic carbon (Thornton, 2002, Mari
438 et al. 2017).

439 As a biological response, it is expected than NP alter total TEP concentration as
440 previously reported in presence of MP (Lagarde et al., 2016). Recently, Bergami et al.
441 (2016) suggested that presence of NP promotes the formation of rounded aggregates of
442 PS-NH₂ around algae cells probably due to the presence of organic matter and/or the
443 EPS in the media. Nevertheless, this hypothesis was based on scanning electronic
444 microscopy (SEM) images of glutaraldehyde fixed cells not taking into account TEP
445 measurements. Based on the microscopic observations performed in this study on fresh
446 and pseudo-lugol fixated cells, it seems that pseudo-lugol fixation promotes aggregation
447 in the media probably associated to the presence of TEP, not only in NP exposed
448 cultures but also in control ones. Then, microscopy approach could be misleading to
449 evidence NP influence on TEP presence and we advocate quantifying TEP as done here
450 by spectrophotometric measurement. Our data revealed a significant decrease in total

451 TEP ($\mu\text{g Xeq L}^{-1}$) at high NP concentration during exponential growth. Such decrease
452 could be explained by a general decrease of the EPS producer diatoms and bacteria: i)
453 we observed reduction (62 % down) of algae' cellular growth in this treatment and ii)
454 we observed reduction (30.5 % down) in bacteria concentration in comparison to
455 control. Indeed, it is difficult to discriminate the origin of TEP. Some carbohydrates are
456 diatoms-specific, and measurements of dissolved carbohydrates in the culture would be
457 a way to discriminate diatom TEP from bacterial one. However the observed difference
458 between the total TEP concentrations at the end of the experiment for high NP exposure
459 disappeared when TEP concentration is normalized to diatom cell concentrations,
460 suggesting that in our experiment diatom may be the main producer of TEP.

461

462 **NP impair major physiological traits of diatoms at exponential growth**

463 Exponential cultures are characterized by a fast growth which leads to intense
464 duplication of chloroplasts, nucleus, Golgi apparatus and mitochondria requiring high
465 amounts of energy (Tanaka et al., 2015). They also duplicate their frustules from which
466 two new cells are produced (Pickett-Heaps, 1998) therefore promoting membrane
467 exhibition to NP which may increase their susceptibility to NP exposure. The adsorption
468 of PS-NH₂ onto *Dunaliella tertiolecta* membranes has been reported previously
469 (Bergami et al., 2017). Furthermore, higher adsorption ratio of PS-NH₂ as compared to
470 other functionalized groups such as PS-COOH or non-functionalized polystyrene
471 particles has been reported (Nolte et al., 2017). Such high adsorption of PS-NH₂ also
472 evidenced *in vitro* with mammalian cells (Anguissola et al., 2014; Varela et al., 2012)
473 was justified by the attraction of positively charged particles with negatively charged
474 membrane lipids (Rossi and Monticelli, 2016). Nevertheless, diatoms are covered by a
475 silica frustule, which can protect the membranes against potential external stressors such
476 as NP. Recently, Walsh et al. (2017) have reported that -NH₂ groups have high affinity
477 to frustule's silica in diatoms. This fits with the observed increase in FSC and SSC
478 suggesting cell surface changes upon NP exposure in exponential cultures. It may be
479 explained by a rapid adhesion of NP to algal cell surface as evidenced by SEM. Indeed,
480 increase in light diffraction upon NP adsorption on the cell surface was previously
481 reported in other cells types, *i.e.* gametes (González-Fernández et al., 2018). Particles
482 adhered onto the algae' cells could also enhance light attenuation and reduce the
483 availability of nutrient and gas exchange, which may consequently trigger adverse

484 effects on algae respiration and photosynthesis (Bergami et al., 2016; Bhattacharya et
485 al., 2010).

486 In this work, NP significantly impacted the photosynthetic machinery of microalgae
487 cultures in exponential phase. A decrease in photosynthesis activity in microalgae upon
488 exposure to NP was already reported (Bergami et al., 2017; Bhattacharya et al., 2010;
489 Mao et al., 2018). Particularly, decrease in photosynthetic efficiency was expected after
490 exposure to positively charged NP because they are tightly absorbed on cellulosic
491 membranes of microalgae (Nolte et al., 2017). The excessive cell surface coverage by
492 PS-NH₂ is likely to inhibit photosynthesis and/or disrupt cell wall (Nolte et al., 2017).
493 Loss of membrane integrity could also explain the decrease in algal metabolic activity
494 (esterase activity). Plant and other photosynthetic organisms use chlorophyll to absorb
495 light and convert it into chemical energy. The dose-dependent reduction of chlorophyll
496 content in cultures in exponential phase suggests a high sensitiveness of thylakoid
497 photosynthetic machinery with however only a moderate impact on photosynthetic
498 efficiency at high NP exposure in our experimental conditions. Overall, it is proposed
499 that NP exposure may impair the diatoms energy intake by affecting chloroplast
500 integrity.

501 **NP triggered an increase of ROS production by algae at both growing phases**

502 In photosynthetic organisms, ROS are continuously produced as by-products through
503 various metabolic pathways localized in mitochondria, chloroplasts and peroxisomes,
504 (Liu et al., 2007). Enhancement of ROS production after exposure to NP has been
505 previously observed (Bhattacharya et al., 2010; Mao et al., 2018), as well as in this
506 study at two culture phases strengthening its status of ubiquitous stress response.
507 Impairment of the electron transport chain in chloroplasts may results in electron
508 accumulation increasing the ROS level. It is also noteworthy that ROS production was
509 the unique parameter affected in stationary cultures, even at low NP dose. This suggests
510 that ROS generation upon NP exposure may constitute a predominant mechanism
511 leading to nano-toxicity, as reported by Fu et al. (2014). The impairment of the
512 photosynthetic machinery together with the increase in ROS levels could lead to
513 membrane lipid peroxidation as previously described by Mao et al. (2018) promoting
514 cell damage and reducing cell growth.

515 **5. Conclusion**

516 In natural environments, all growing states coexist, making difficult to predict the
517 impact of NP on diatoms community and on organisms at higher trophic levels.
518 Ecological effects of NP may indeed occur higher up in the food web, with algae-
519 particle interaction as the first step in the biomagnification (Nolte et al., 2017 ; Navarro
520 et al., 2008) as previously shown in suspension-feeding bivalves (Ward and Kach,
521 2009). Differences in TEP concentration according to growth phase can be a key
522 parameter affecting the fate and toxicity of NP on marine diatoms. This work using
523 fairly realistic environmental scenario of nanoplastics pollution highlights the
524 importance of taking into account algae growing phases when evaluating the impact of
525 plastic in phytoplankton ecotoxicological studies. Further research focusing on the
526 interaction of NP with cellular membranes as well as the impairment of the
527 photosynthesis machinery are of great interest for deeply understanding the global
528 diatoms' responses to plastic contamination.

529 **Acknowledgements**

530 The authors are grateful to Philippe Miner from Ifremer for his assistance during
531 phytoplankton culture, to Dr. Philippe Elies for the microscopy observations and Olivier
532 Lozach from the COSM team at the University of Western Brittany for DLS
533 measurements. We thank Helen McCombie for her help in editing the English.

534 **Funding sources**

535 This work was supported by the NANO Project (ANR-15-CE34-0006-02) funded by the
536 French Agence Nationale de la Recherche (ANR).

537 **References**

- 538 Allard, B., Tazi, A., 1993. Influence of growth status on composition of extracellular
539 polysaccharides from two *Chlamydomonas* species. *Phytochemistry* 32, 41-47.
- 540 Anguissola, S., Garry, D., Salvati, A., O'Brien, P.J., Dawson, K.A., 2014. High content
541 analysis provides mechanistic insights on the pathways of toxicity induced by
542 amine-modified polystyrene nanoparticles. *PLoS One* 9.
543 <https://doi.org/10.1371/journal.pone.0108025>
- 544 Azetsu-Scott, K., Passow, U. 2004. Ascending marine particles: Significance of
545 transparent exopolymer particles (TEP) in the upper ocean. *Limnol. Oceanogr.* 49,

- 546 741–748.
- 547 Bergami, E., Pugnolini, S., Vannuccini, M.L., Manfra, L., Faleri, C., Savorelli, F.,
548 Dawson, K.A., Corsi, I., 2017. Long-term toxicity of surface-charged polystyrene
549 nanoplastics to marine planktonic species *Dunaliella tertiolecta* and *Artemia*
550 *franciscana*. *Aquat. Toxicol.* 189, 159–169.
551 <https://doi.org/10.1016/j.aquatox.2017.06.008>
- 552 Bergmann, M., Wirzberger, V., Krumpfen, T., Lorenz, C., Primpke, S., Tekman, M.B., et
553 al. 2017. High quantities of microplastic in Arctic deep-sea sediments from the
554 HAUSGARTEN Observatory. *Envir. Sci. Technol.* 51, 11000–11010. doi:
555 10.1021/acs.est.7b03331
- 556 Bistricki, T., Munawar, M. 1978. A rapid preparation method for scanning electron
557 microscopy of Lugol preserved algae. *J. Microsc.* 114, 215–218. Bhattacharya, P.,
558 Lin, S., Turner, J.P., Ke, P.C., 2010. Physical adsorption of charged plastic
559 nanoparticles affects algal photosynthesis. *J. Phys. Chem. C* 114, 16556–16561.
560 <https://doi.org/10.1021/jp1054759>
- 561 Canesi, L., Balbi, T., Fabbri, R., Salis, A., Damonte, G., Volland, M., Blasco, J., 2017.
562 Biomolecular coronas in invertebrate species: Implications in the environmental
563 impact of nanoparticles. *NanoImpact* 8, 89–98.
564 <https://doi.org/10.1016/j.impact.2017.08.001>
- 565 Cole, M., Galloway, T.S., 2015. Ingestion of nanoplastics and microplastics by Pacific
566 oyster larvae. *Environ. Sci. Technol.* 49, 14625–14632. [https://doi.org/10.1021/](https://doi.org/10.1021/acs.est.5b04099)
567 [acs.est.5b04099](https://doi.org/10.1021/acs.est.5b04099).
- 568 Corzo, A., Morillo, J.A., Rodríguez, S., 2000. Production of transparent exopolymer
569 particles (TEP) in cultures of *Chaetoceros calcitrans* under nitrogen limitation.
570 *Aquat. Microb. Ecol.* 23, 63–72. <https://doi.org/10.3354/ame023063>
- 571 Datta, M. S., Sliwerska, E., Gore, J., Polz, M. F., and Cordero, O. X. 2016. Microbial
572 interactions lead to rapid micro-scale successions on model marine particles. *Nat.*
573 *Commun.* 7:11965. doi: 10.1038/ncomms11965
- 574 Dubaish, F., and Liebezeit, G. 2013. Suspended microplastics and black carbon particles
575 in the Jade system, southern North Sea. *Water, Air, Soil, Poll.* 224, 1352. doi:

- 576 10.1007/s11270-012-1352-9
- 577 Erni-Cassola, G., Gibson, M.I., Thompson, R.C., christie-oleza, J., 2017. Lost, but
578 found with Nile red; a novel method to detect and quantify small microplastics (20
579 μm –1 mm) in environmental samples. *Environ. Sci. Technol.*, 2017, 51 (23),
580 13641–13648
- 581 Fabra, M.J., Busolo, M.A., Lopez-Rubio, A., Lagaron, J.M., 2013. Nanostructured
582 bilayers in foodpackaging. *Trends Food Sci. Technol.* 31, 79–87
- 583 FAO. 2017. Microplastics in fisheries and aquaculture.
- 584 Field, C.B., Behrenfeld, M.J., Randerson, J.T., Falkowski, P., 1998. Primary production
585 of the biosphere: integrating terrestrial and oceanic components. *Science* 281
586 (5374), 237–240
- 587 Fu, P.P., Xia, Q., Hwang, H., Ray, P.C., Yu, H., 2014. Mechanisms of nanotoxicity:
588 Generation of reactive oxygen species. *J. Food Drug Anal.* 22, 64–75.
589 <https://doi.org/10.1016/j.jfda.2014.01.005>
- 590 Galloway, T.S., Cole, M., Lewis, C., 2017. Interactions of microplastic debris
591 throughout the marine ecosystem. *Nat. Ecol. Evol.* 1, 1–16.
592 <https://doi.org/10.1038/s41559-017-0116>
- 593 Garvey, M., Moriceau, B., and Passow, U. 2007. Applicability of the FDA assay to
594 determine the viability of marine phytoplankton under different environmental
595 conditions. *Mar. Ecol. Prog. Ser.* 352, 17–26. doi:10.3354/meps07134.
- 596 GESAMP. 2016. “Sources, fate and effects of microplastics in the marine environment:
597 part two of a global assessment” (Kershaw, P.J., and Rochman, C.M., eds).
598 (IMO/FAO/UNESCO-IOC/UNIDO/WMO/IAEA/UN/UNEP/UNDP Joint Group
599 of Experts on the Scientific Aspects of Marine Environmental Protection). Rep.
600 Stud. GESAMP No. 93, 220 p.
- 601 Gigault, J., Pedrono, B., Maxit, B., Ter Halle, A., 2016. Marine plastic litter: the
602 unanalyzed nano-fraction. *Environ. Sci. Nano* 3, 346–350.
603 <https://doi.org/10.1039/C6EN00008H>

- 604 Gigault, J., Ter Halle, A., Baudrimont, M., Pascal, P.-Y., Gauffre, F., Phi, T.-L., et al.
605 2018. Current opinion: what is a nanoplastic? *Environ. Pollut.* 230, 1030–1034.
606 doi: 10.1016/j.envpol.2018.01.024
- 607 González-Fernández, C., Tallec, K., Le Goïc, N., Lambert, C., Soudant, P., Huvet, A.,
608 Suquet, M., Berchel, M., Paul-Pont, I., 2018. Cellular responses of Pacific oyster
609 (*Crassostrea gigas*) gametes exposed *in vitro* to polystyrene nanoparticles.
610 *Chemosphere* 208, 764–772. <https://doi.org/10.1016/j.chemosphere.2018.06.039>
- 611 Hernandez, L. M., Yousefi, N., Tufenkji, N. 2017. Are There Nanoplastics in Your
612 Personal Care Products? *Environmental Science & Technology Letters*, 4(7), 280–
613 285. <https://doi.org/10.1021/acs.estlett.7b00187>
- 614 Huvet, A., Paul-Pont, I., Fabioux, C., Lambert, C., Suquet, M., Thomas, Y., ...
615 Sussarellu, R. (2016). Reply to Lenz et al.: Quantifying the smallest microplastics
616 is the challenge for a comprehensive view of their environmental impacts.
617 *Proceedings of the National Academy of Sciences*, 113(29), E4123–E4124.
618 <https://doi.org/10.1073/pnas.1607221113>
- 619 Khowala, S., Verma, D., Banik, S.P., 2008. Biomolecules: Introduction, Structure &
620 Function -Carbohydrates[online]. Indian Institute of Chemical Biology
621 [http://www.academia.edu/1114817/Biomolecules_Introduction_Structure_and](http://www.academia.edu/1114817/Biomolecules_Introduction_Structure_and_Functions_-_Carbohydrates)
622 [Functions - Carbohydrates.](http://www.academia.edu/1114817/Biomolecules_Introduction_Structure_and_Functions_-_Carbohydrates)
- 623 Kroll, A., Behra, R., Kaegi, R., Sigg, L. 2014. Extracellular polymeric substances (EPS)
624 of freshwater biofilms stabilize and modify CeO₂ and Ag nanoparticles. *Plos One*
625 9(10), e110709
- 626 Lagarde, F., Olivier, O., Zanella, M., Daniel, P., Hiard, S., Caruso, A., 2016.
627 Microplastic interactions with freshwater microalgae: Hetero-aggregation and
628 changes in plastic density appear strongly dependent on polymer type. *Environ.*
629 *Pollut.* 215, 331–339. <https://doi.org/10.1016/j.envpol.2016.05.006>
- 630 Lambert, S., Wagner, M., 2016. Characterisation of nanoplastics during the degradation
631 of polystyrene. *Chemosphere* 145, 265–268.
632 <https://doi.org/10.1016/j.chemosphere.2015.11.078>

- 633 Lenz, R., Enders, K., & Nielsen, T. G. (2016). Microplastic exposure studies should be
634 environmentally realistic. *Proceedings of the National Academy of Sciences*,
635 113(29), E4121–E4122. <https://doi.org/10.1073/pnas.1606615113>
- 636 Liu, W.; Au, D. W. T.; Anderson, D. M.; Lam, P. K. S.; Wu, R. S. S. Effects of
637 nutrients, salinity, pH and light:dark cycle on the production of reactive oxygen
638 species in the alga *Chattonella marina*. *J. Exp. Mar. Biol. Ecol.* 2007, 346, 76-86
- 639 Long, M., Moriceau, B., Gallinari, M., Lambert, C., Huvet, A., Raffray, J., Soudant, P.,
640 2015. Interactions between microplastics and phytoplankton aggregates: Impact on
641 their respective fates. *Mar. Chem.* 175, 39–46.
642 <https://doi.org/10.1016/j.marchem.2015.04.003>
- 643 Long, M., Paul-Pont, I., Hégaret, H., Moriceau, B., Lambert, C., Huvet, A., Soudant, P.,
644 2017. Interactions between polystyrene microplastics and marine phytoplankton
645 lead to species-specific hetero-aggregation. *Environ. Pollut.* 228, 454–463.
646 <https://doi.org/10.1016/j.envpol.2017.05.047>
- 647 Malviya, S., Scalco, E., Audic, S., Vincent, F., Veluchamy, A., Poulain, J. 2016.
648 Insights into global diatom distribution and diversity in the world's ocean. *Proc.*
649 *Natl. Acad. Sci.*, 201509523.
- 650 Manfra, L., Rotini, A., Bergami, E., Grassi, G., Faleri, C., Corsi, I., 2017. Comparative
651 ecotoxicity of polystyrene nanoparticles in natural seawater and reconstituted
652 seawater using the rotifer *Brachionus plicatilis*. *Ecotoxicol. Environ. Saf.* 145,
653 557–563. <https://doi.org/10.1016/j.ecoenv.2017.07.068>
- 654 Marie, D., F. Partensky, S. Jacquet, D. Vaultot. 1997. Enumeration and Cell Cycle
655 Analysis of Natural Populations of Marine Picoplankton by Flow Cytometry Using
656 the Nucleic Acid Stain SYBR Green I. *Appl. Environ. Microbiol.* 63, 1. 186-93.
- 657 Mari, X., Passow, U., Migon, C., Burd, A.B., Legendre, L., 2017. Transparent
658 exopolymer particles: Effects on carbon cycling in the ocean. *Prog. Oceanogr.* 151,
659 13–37. <https://doi.org/10.1016/j.pocean.2016.11.002>
- 660 Mao, Y., Ai, H., Chen, Y., Zhang, Z., Zeng, P., Kang, L., Li, W., Gu, W., He, Q., Li, H.,
661 2018. Phytoplankton response to polystyrene microplastics: Perspective from an

- 662 entire growth period. *Chemosphere* 208, 59–68.
663 <https://doi.org/10.1016/j.chemosphere.2018.05.170>
- 664 Merinska, D., Dujkova, Z., 2012. Polystyrene (nano) composites with possible anti-
665 bacterial effect. *Mathematical Methods and Techniques in Engineering and*
666 *Environmental Science* (ISBN: 978-1-61804-046-6).
- 667 Mopper, K., Zhou, J., Ramana, K. S., Passow, U., Dam, H. G., & Drapeau, D. T. 1995.
668 The role of surface-active carbohydrates in the flocculation of a diatom bloom in a
669 mesocosm. *Deep-Sea Research II*, 42,47–73
- 670 Navarro, E., Baun, A., Behra, R., Hartmann, N.B., Filser, J., Miao, A.J., Quigg, A.,
671 Santschi, P.H., Sigg, L., 2008. Environmental behavior and ecotoxicity of
672 engineered nanoparticles to algae, plants, and fungi. *Ecotoxicology* 17, 372–386.
673 <https://doi.org/10.1007/s10646-008-0214-0>
- 674 Nolte, T.M., Hartmann, N.B., Kleijn, J.M., Garnæs, J., van de Meent, D., Jan Hendriks,
675 A., Baun, A., 2017. The toxicity of plastic nanoparticles to green algae as
676 influenced by surface modification, medium hardness and cellular adsorption.
677 *Aquat. Toxicol.* 183, 11–20. <https://doi.org/10.1016/j.aquatox.2016.12.005>
- 678 Passow, U., 2002. Transparent Exopolymer Particles in Aquatic Environments. *Prog.*
679 *Oceanogr.* 55, 287–333. [https://doi.org/10.1016/S0079-6611\(02\)00138-6](https://doi.org/10.1016/S0079-6611(02)00138-6)
- 680 Passow, U., and Alldredge, A. L. 1995. A dye-binding assay for the spectrophotometric
681 measurement of transparent exopolymer particles (TEP). *Limnol. Oceanogr.* 40,
682 1326–1335. doi:10.4319/lo.1995.40.7.1326.
- 683 Passow, U., De La Rocha, C.L. 2006. Accumulation of mineral ballast on organic
684 aggregates. *Glob. Biogeochem. Cycles.*20(1), 10-13.
- 685 Paul-Pont, I., Tallec, K., Gonzalez-Fernandez, C., Lambert, C., Vincent, D., Mazurais,
686 D., Zambonino-Infante, J.-L., Brotons, G., Lagarde, F., Fabioux, C., Soudant, P.,
687 Huvet, A., 2018. Constraints and Priorities for Conducting Experimental
688 Exposures of Marine Organisms to Microplastics. *Front. Mar. Sci.* 5, 1–22.
689 <https://doi.org/10.3389/fmars.2018.00252>
- 690 Pickett-Heaps, J.D., 1998. Cell Division and Morphogenesis of the Centric Diatom

- 691 *Chaetoceros Decipiens* (Bacillariophyceae) Ii. Electron Microscopy and a New
692 Paradigm for Tip Growth. *J. Phycol.* 34, 995–1004. [https://doi.org/10.1046/j.1529-](https://doi.org/10.1046/j.1529-8817.1998.340995.x)
693 [8817.1998.340995.x](https://doi.org/10.1046/j.1529-8817.1998.340995.x)
- 694 Peeken, I., Primpke, S., Beyer, B., Gütermann, J., Katlein, C., Krumpfen, T., 2018.
695 Arctic sea ice is an important temporal sink and means of transport for
696 microplastic. *Nat. Commun.* 9, 2041–1723. doi: 10.1038/s41467-018-03825-5
- 697 *Plastics Europe 2017. An analysis of European plastics production, demand and waste*
698 *data. Technical Report.*
699 https://www.plasticseurope.org/application/files/5715/1717/4180/Plastics_the_facts_2017_FINAL_for_website_one_page.pdf
700
- 701 Rogach, A., Susha, A., Caruso, F., Sukhorukov, G., Kornowski, A., Kershaw, S.,
702 Möhwald, H., Eychmüller, A., Weller, H., 2000. Nano- and microengineering: 3-D
703 colloidal photonic crystals prepared from sub- μm -sized polystyrene latex spheres
704 pre-coated with luminescent polyelectrolyte/nanocrystal shells. *Adv. Mater.* 12,
705 333–337.
- 706 Rossi, G., Monticelli, L., 2016. Simulating the interaction of lipid membranes with
707 polymer and ligand-coated nanoparticles. *Adv. Phys.* X 1, 276–296.
708 <https://doi.org/10.1080/23746149.2016.1177468>
- 709 Sjollema, S.B., Redondo-Hasselerharm, P., Leslie, H.A., Kraak, M.H.S., Vethaak, A.D.,
710 2016. Do plastic particles affect microalgal photosynthesis and growth? *Aquat.*
711 *Toxicol.* 170, 259–261. <https://doi.org/10.1016/j.aquatox.2015.12.002>
- 712 Smith, D. C., Steward, G. F., Long, R. A., & Azam, F. 1995. Bacterial mediation of
713 carbon fluxes during a diatom bloom in a mesocosm. *Deep-Sea Research II*,
714 42,75–97
- 715 Strasser, J.R., Srivastava, A., Tsimilli-Michael, M., 2000. The fluorescence transient as
716 a tool to characterize and screen photosynthetic samples, in: *Probing*
717 *Photosynthesis: Mechanism, Regulation & Adaptation.* pp. 445–483.
- 718 Summers, S., Henry, T., Gutierrez, T., 2018. Agglomeration of nano- and microplastic
719 particles in seawater by autochthonous and de novo-produced sources of
720 exopolymeric substances. *Mar. Pollut. Bull.* 130, 258–267.

- 721 <https://doi.org/10.1016/j.marpolbul.2018.03.039>
- 722 Tallec, K., Huvet, A., Di Poi, C., González-Fernández, C., Lambert, C., Petton, B., Le
723 Goïc, N., Berchel, M., Soudant, P., Paul-Pont, I., 2018. Nanoplastics impaired
724 oyster free living stages, gametes and embryos. *Environ. Pollut.* 242, 1226–1235.
725 <https://doi.org/10.1016/j.envpol.2018.08.020>
- 726 Tanaka, A., De Martino, A., Amato, A., Montsant, A., Mathieu, B., Rostaing, P.,
727 Tirichine, L., Bowler, C., 2015. Ultrastructure and Membrane Traffic During Cell
728 Division in the Marine Pennate Diatom *Phaeodactylum tricornutum*. *Protist* 166,
729 506–521. <https://doi.org/10.1016/j.protis.2015.07.005>
- 730 Ter Halle, A., Jeanneau, L., Martignac, M., Jardé, E., Pedrono, B., Brach, L., Gigault, J.,
731 2017. Nanoplastic in the North Atlantic Subtropical Gyre. *Environ. Sci. Technol.*
732 *acs.est.7b03667*. <https://doi.org/10.1021/acs.est.7b03667>
- 733 Thornton, D.C.O., 2002. Diatom aggregation in the sea: Mechanisms and ecological
734 implications. *Eur. J. Phycol.* 37, 149–161.
735 <https://doi.org/10.1017/S0967026202003657>
- 736 Varela, J.A., Bexiga, M.G., Åberg, C., Simpson, J.C., Dawson, K.A., 2012. Quantifying
737 size-dependent interactions between fluorescently labeled polystyrene
738 nanoparticles and mammalian cells. *J. Nanobiotechnology* 10, 39.
739 <https://doi.org/10.1186/1477-3155-10-39>
- 740 Velev, O.D., Kaler, E.W., 1999. In situ assembly of colloidal particles into miniaturized
741 biosensors. *Langmuir* 15, 3693–3698. <http://dx.doi.org/10.1021/la981729c>.
- 742 Verity, P.G., Whipple, S.J., Nejstgaard, J.C., Aldrekamp, A.C. 2007. Colony, size, cell
743 number, carbon and nitrogen content of *Phaeocystis pouchetii* from western
744 Norway. *J. Plankton. Res.* 4, 359-367.
- 745 Walne, P. R., 1966. Experiments in the Large-scale Culture of the Larvae of *Ostrea*
746 *edulis* L. 848 Fishery In, Her Majesty's Stationery Office, London.
- 747 Walsh, P.J., Clarke, S.A., Julius, M., Messersmith, P.B., 2017. Exploratory Testing of
748 Diatom Silica to Map the Role of Material Attributes on Cell Fate. *Sci. Rep.* 7, 1–
749 13. <https://doi.org/10.1038/s41598-017-13285-4>

- 750 Ward, J.E., Kach, D.J., 2009. Marine aggregates facilitate ingestion of nanoparticles by
751 suspension-feeding bivalves. *Mar. Environ. Res.* 68, 137e142. [http://](http://dx.doi.org/10.1016/j.marenvres.2009.05.002)
752 dx.doi.org/10.1016/j.marenvres.2009.05.002.
- 753 Yokota, K., Waterfield, H., Hastings, C., Davidson, E., Kwietniewski, E., Wells, B.,
754 2017. Finding the missing piece of the aquatic plastic pollution puzzle: Interaction
755 between primary producers and microplastics. *Limnol. Oceanogr. Lett.* 2, 91–104.
756 <https://doi.org/10.1002/lol2.10040>
- 757 Zhao, S., Danley, M., Ward, J. E., Li, D., and Mincer, T. J. 2017. An approach for
758 extraction, characterization and quantitation of microplastic in natural marine snow
759 using Raman microscopy. *Anal. Methods* 9, 1470–1478.
760 [doi:10.1039/C6AY02302A](https://doi.org/10.1039/C6AY02302A).
- 761 Zhou, J., Mopper, K., Passow, U. 1998. The role of surface-active carbohydrates in the
762 formation of transparent exopolymer particles (TEP) by bubble adsorption of
763 seawater. *Limnol. Oceanogr.* 43, 1860-1871
- 764 Zettler, E. R., Mincer, T. J., and Amaral-Zettler, L. A. 2013. Life in the “Plastisphere”:
765 microbial communities on plastic marine debris. *Envir. Sci. Technol.* 47, 7137–
766 7146. [doi: 10.1021/es401288x](https://doi.org/10.1021/es401288x)

FIGURE CAPTIONS

Figure 1. Nanoplastics characterization using Dynamic Light Scattering in ultrapure water (A), filtered seawater (B), filtered algal media at exponential phase (C) filtered algal media at stationary phase (D) and Transmission Electronic Microscopy (TEM) imaging in ultrapure water (E). Size distribution of 50 nm PS-NH₂ measured in triplicates (corresponding to the different colors: green, red, blue) using a Zetasizer Nano Series software 6.2. TEM observations of 50 nm PS-NH₂ are also presented. Scale bar: 20 nm.

Figure 2. Scanning electron micrographs of *Chaetoceros neogracile* exponential cells in control (A, B) and after 72h exposure to high NP concentration (5 µg mL⁻¹ PS-NH₂) (C, D). Samples were processed in fresh. Exposed cells presented high amount of PS-NH₂ particles attached onto the cell surface. Scale bar: 5µm (A, C) and 1µm (B, D).

Figure 3. Diatom cellular parameters affected by PS-NH₂ exposure at exponential phase: cellular growth (A), relative cell complexity (Side scatter SSC) (B), relative cell size (forward scatter FSC) (C), chlorophyll content (red fluorescence) (D), photosynthesis activity (E), esterase activity (green fluorescence) (F), intracellular ROS production (G) and bacteria concentration (H). Data are presented as means (n=3) ± SD. Significant level marked at p< 0.05. Lowercase letters indicate differences between treatments within the same exposure time (1-way-ANOVA analysis).

Figure 4. Transparent Exopolymer Particles (TEP) concentration measured before exposure (A, B) and after 96 h exposure to nanoplastics (C, D). A,C: TEP expressed by microgram of Gum Xanthan equivalent per liter (µg Xeq L⁻¹) and B,D: TEP expressed by microgram of Gum Xanthan equivalent per cell (µg Xeq cell⁻¹). Data are presented as means (n=3) ± SD. Significant level marked at p< 0.05. Lowercase letters indicate differences between treatments within the same exposure time (1-way-ANOVA analysis).

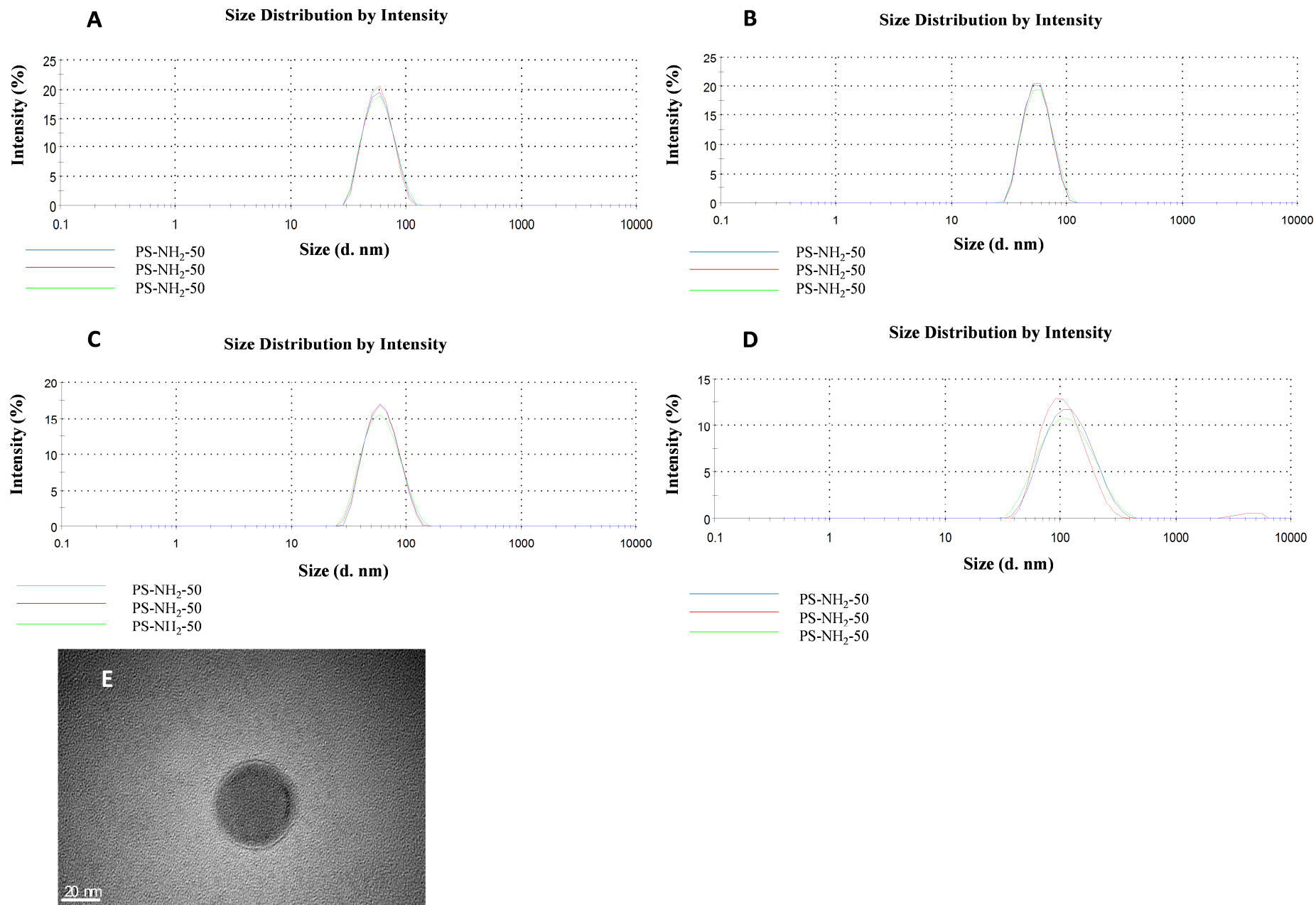


Figure 1.

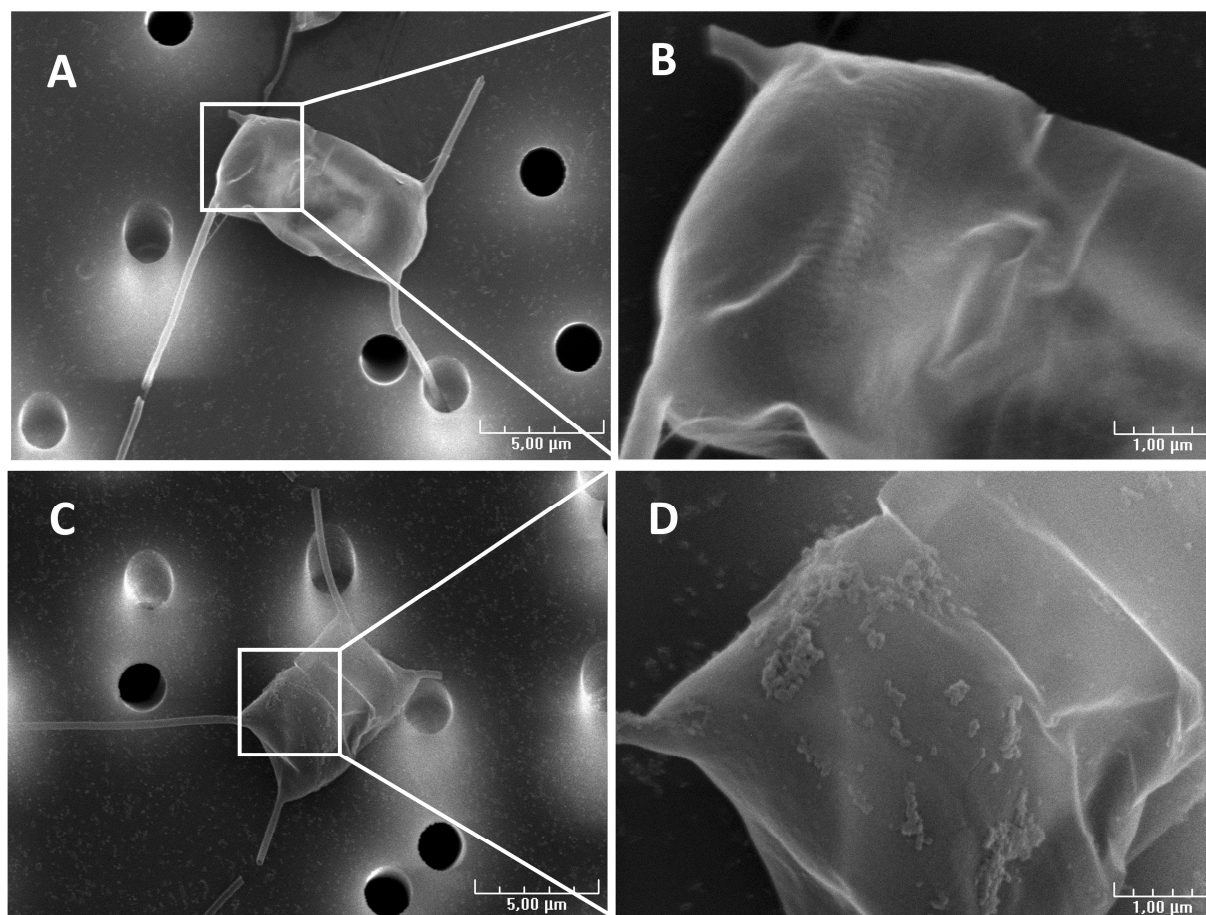


Figure 2.

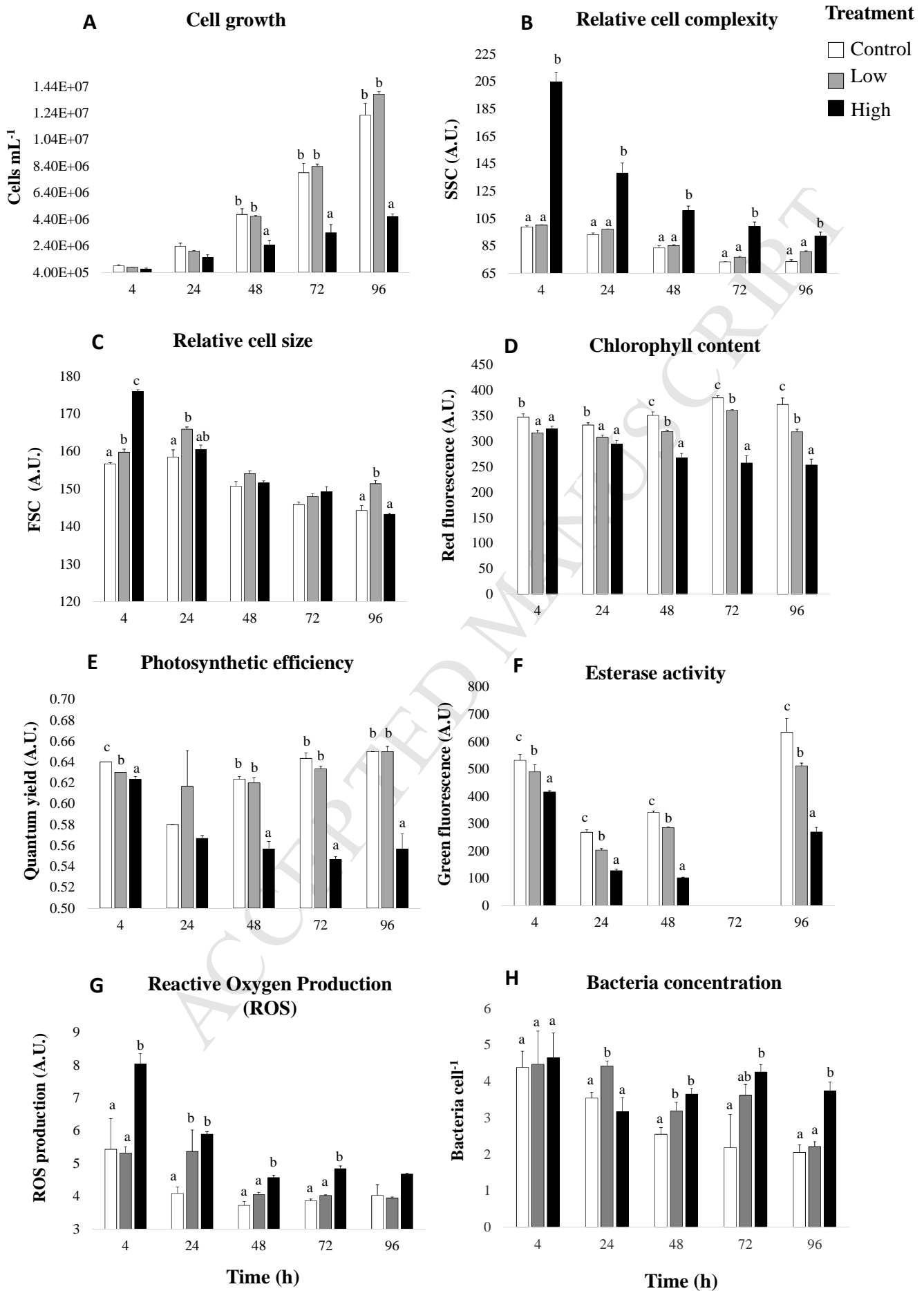


Figure 3.

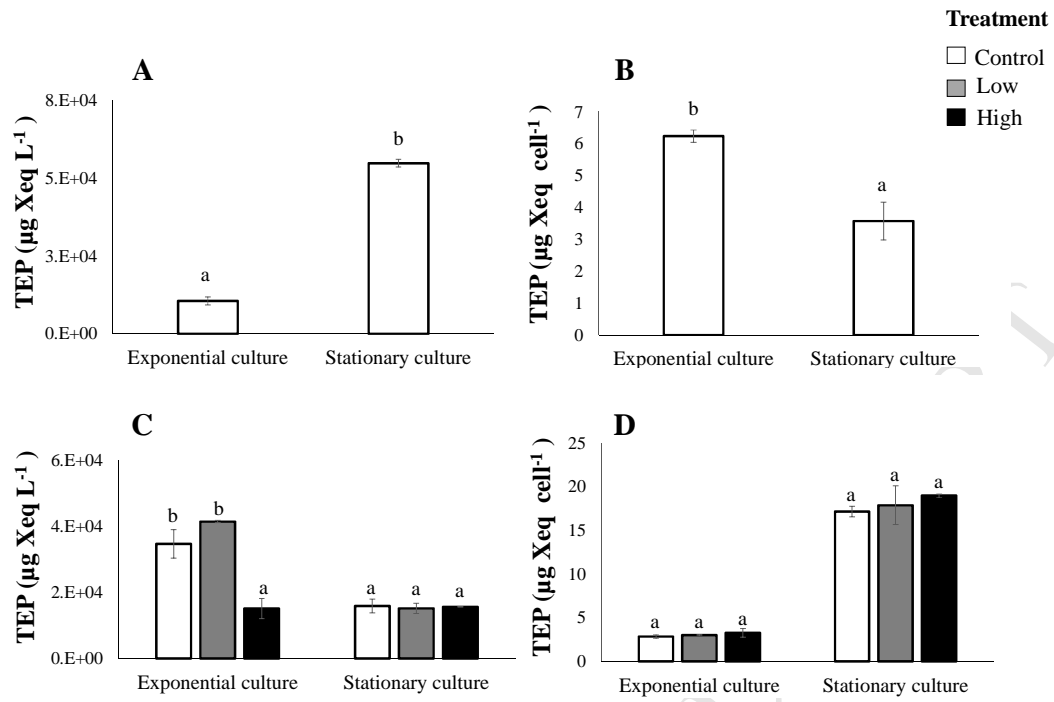


Figure 4.

Highlights

1. Interaction of NP and diatoms was studied at exponential and stationary phases
2. Transparent Exopolymer Particles (TEP) alter NP fate by aggregating NP
3. NP impairs major physiological traits of diatoms at exponential phase
4. Whatever the aggregation state, NP promotes oxidative stress at both growth phases